

## Pulse Detection and Processing in TES Detectors

M.T. Ceballos,<sup>1</sup> B. Cobo,<sup>1</sup> R. Fraga-Encinas,<sup>1</sup> J. van der Kuur,<sup>2</sup> and J. Schuurmans<sup>2</sup>

<sup>1</sup>*Instituto de Física de Cantabria (CSIC-UC), Avda. de Los Castros s/n, 39005 Santander, Spain*

<sup>2</sup>*Netherlands Institute for Space Research, Sorbonnelaan 2, 3584 CA Utrecht, The Netherlands*

### Abstract.

We present here the computational basis of the software chain (XRAYCHAIN) developed to detect and analyze the pulses generated in Transition Edge Sensors (TES) devices in response to the incoming X-ray astronomical photons. The final objective of this analysis is the obtention of the arrival time, position and energy content of the photons, that will enable the study and characterization of the observed source.

This code is currently being developed under a collaboration between IFCA (Spain) and SRON (NL) institutes, as part of a larger project named EURECA (de Korte et al. 2009) involving many other institutes in Europe and the USA. This project was created to design the TES prototype proposed for the XEUS ESA mission, that has currently evolved into the ATHENA mission.

## 1. Introduction

The ATHENA (Advanced Telescope for High ENergy Astrophysics) mission, currently under study by the European Space Agency (ESA), will carry on board an X-ray imaging calorimeter spectrometer (XMS) based on Transition Edge Sensor (TES) technology.

In these type of devices, the incoming astronomical X-ray photons are absorbed by the detector, increasing its temperature and giving rise to current pulses as a result of an abrupt resistance increment. The arrival time, position and energy content of the pulses are then obtained by analyzing the electrical pulses generated.

We have designed a full suite of software tools (Ceballos et al. 2011) to detect the pulses generated in this type of devices in response to the incoming X-ray photons as well as to characterize the TES instrument. As part of this package, we present here the XRAYCHAIN, the subset of tasks aimed at pulse detection and analysis.

## 2. XRAYCHAIN

This software chain comprises five individual C++ tasks (trigger, pulshape, filter, energyresol and holzgauss) developed for the maximization of pulse detection capabilities and the calculation of the energy content of the pulses. In addition, the energy resolution of the device is determined for calibration purposes.

The input file of this pipeline is a FITS file containing the values of the detector response (a current) as a function of time. The output comprises a list of intermediate and final FITS files with the list of pulses that have been detected, their arrival and end times and their energy content. In addition, the chain gives the energy resolution of the detector.

Currently, the software is designed for a single pixel detector, which will be extended in the future to analyze the output of a multipixel detector. In that case, it will also determine the arrival position of the X-ray photons.

In the following subsections we will describe the purpose of each of these processing tasks and the algorithms designed to get the required functionality.

## 2.1. trigger

The aim of this task is to find (in the noisy response of the TES detector) the current (I) pulses generated by the X-ray incoming photons and to determine their starting and end points. The algorithm can be divided in 3 steps:

- **Noise reduction:** in order to reduce the noise in the signal, to improve the chances of pulse detection, the input signal is filtered with a low-pass filter (boxcar) with a box length that is an input task parameter (see Fig. 1).

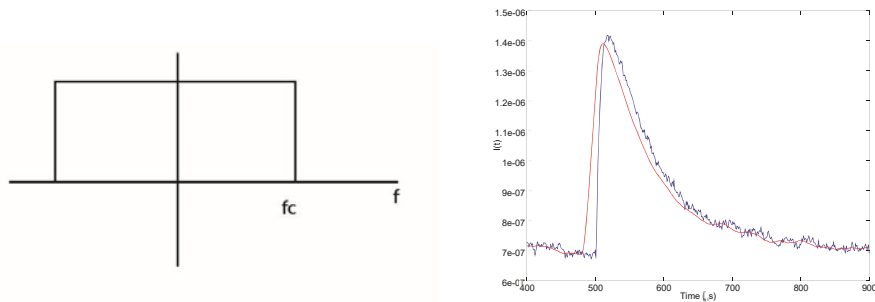


Figure 1. Low-pass filtering process in trigger (Left: low-pass filter. Right: unfiltered pulse in blue and filtered pulse in red).

- **Thresholding of single/large pulses:** since pulses can be very close to each other, the pulse-peak detection is done in the first derivative of the signal through a median kappa-clipping method (see Fig. 2).
- **Adjusted derivative:** since it is possible that the smallest pulses cannot reach the threshold imposed by the largest ones or that they can be masked by these large pulses, an iterative process is performed. This involves subtracting the first derivative of pulses already detected from the global first derivative (adjusted derivative method in Boyce et al. (1999)), then enhancing the smallest signals. This is done until no more pulses are found (see Fig. 2).

## 2.2. pulseshape

The aim of this task is the qualification of the current (I) pulses. The task analyses the pulses and classifies them as single, multiple, saturated, etc.

## PulseDetectioninTES

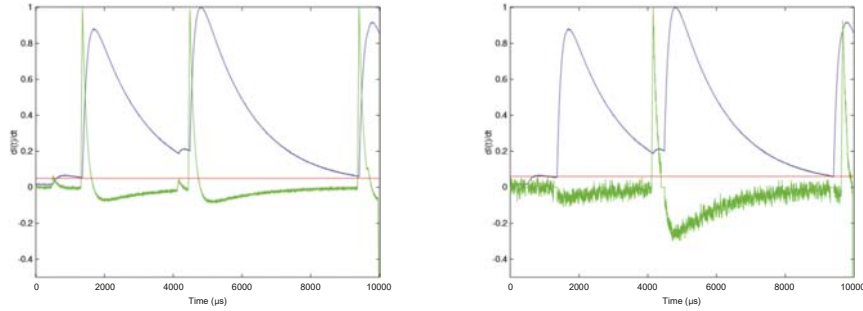


Figure 2. Thresholding of first (left) and “adjusted” (right) derivative: unfiltered pulses in blue, first/adjusted derivative in green and threshold for peak finding in red.

### 2.3. filter

With the list of single pulses this task creates a pulse template in order to, later in the pipeline, convolve it with every current pulse to determine its energy.

### 2.4. energyresol

The energy of every pulse must be calculated by means of the autocorrelation of the pulse signal. However, due to the confusion added by the noise, this process is approximated by the convolution of the pulse ( $I(t)$ ) with the template ( $T(t)$ ) calculated by the task filter. Energyresol calculates the energy of the pulses before calibration (i.e. the *Pseudo Energy*,  $e$ ):

$$e = \text{PseudoEnergy} = \int_{-\infty}^{+\infty} |I(t)|^2 dt \simeq \int_{-\infty}^{+\infty} I(t) * T(t) dt$$

$$E = \text{Energy} = b \cdot e + c \cdot e^2,$$

being  $b, c$  the calibration factors.

### 2.5. holzgauss

Once the values of the *Pseudo Energy* of the pulses have been calculated for each pulse, the histogram of the number of pulses vs. the *Pseudo Energy* is fitted to the expected distribution ( $F(e, b, c)$ ). From this fit the calibration parameters, and thus the calibrated energy, can be determined. A new histogram is then produced with the number of pulses at a given energy ( $E$ ) and a fit is then performed to obtain the energy resolution of the detector from the width of the pulse distribution.

### 3. Test Results

We have performed a preliminary test to evaluate the efficiency of the algorithm for detecting the pulses. For this purpose we have simulated data with a software calorimeter simulator developed by SRON, at four different energies of monochromatic pulses (50 eV, 300 eV, 5000 eV and 12000 eV) and at different source count rates and fall times of the pulses. Since count rate and fall time values are related (i.e. increasing the pulse rate while decreasing the fall time of the pulses by the same factor should not make any difference), we have done the simulations for constant values of the product of the

780

Ceballos et al.

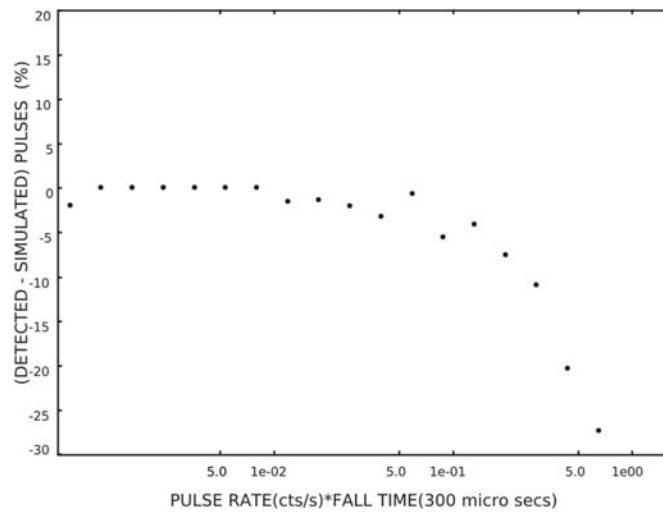


Figure 3. Difference in the number of pulses detected and simulated, vs. an increasing pulse rate. X-axis is the count rate (counts per second) times the fall time of the pulses (s), fixed here to 300 $\mu$ s

count rate by the fall time of the pulses. In figure Fig. 3 there is a plot of the difference between the number of monochromatic pulses simulated and the number of detected pulses (percentage) versus an increasing pulse rate (the fall time of the pulses is fixed here to 300 $\mu$ s). As it can be seen, differences in numbers of pulses are inside the 5% margin almost to a count rate of 1000 counts per second for a single pixel.

Future developments in the code include more intensive tests with the evaluation of the arrival time of the pulses and the energy resolution of the detector, implementation of optimal filtering (including noise spectrum) and energy dependance in the creation of the filter template, and the use of a realistic source of photons in the simulator according to the spectra of real x-ray sources.

**Acknowledgments.** We acknowledge financial support by the Spanish Ministry of Science and Innovation (MICINN) under projects ESP2006-13608-C02-01, AYA200908059 and AYA2010-21490-C02-01.

## References

- Boyce, K. R., et al. 1999, in EUV, X-Ray, and Gamma-Ray Instrumentation for Astronomy X, edited by O. H. Siegmund, & K. A. Flanagan, vol. 3765 of Proc. SPIE, 741
- Ceballos, M., Fraga, R., Cobo, B., van der Kuur, J., Schuurmans, J., Gonzalez, I., & Carrera, F. 2011, in ADASS XX, edited by I. N. Evans, A. Accomazzi, D. J. Mink & A. H. Rots, vol. 1442 of ASP Conf. Ser., 335
- de Korte, P., et al. 2009, in American Astronomical Society Meeting Abstracts #213, vol. 41, 457.14